Polymer Degradation and Stability 118 (2015) 1–9

Contents lists available at ScienceDirect

Polymer Degradation and Stability

journal homepage: www.elsevier.com/locate/polydegstab

Innovative controllable photocatalytic degradation of polystyrene with hindered amine modified aromatic polyamide dendrimer/polystyrene-grafted-TiO_2 photocatalyst under solar light irradiation

Yonglin Lei [a, *], Hong Lei [a], Jichuan Huo [b]

[a] Engineering Research Center of Biomass Materials, Ministry of Education, School of Materials Science and Engineering, Southwest University of Science and Technology, Mianyang 621010, China
[b] Analytical and Testing Center, Southwest University of Science and Technology, Mianyang 621010, China

ARTICLE INFO

Article history:
Received 5 March 2015
Received in revised form
3 April 2015
Accepted 7 April 2015
Available online 16 April 2015

Keywords:
Aromatic polyamide dendrimer
Hindered amine
Photocatalytic degradation
Polystyrene
TiO_2

ABSTRACT

A novel hindered amine modified aromatic polyamide dendrimer/polystyrene-grafted-TiO_2 hybrid photocatalyst (HADPG-TiO_2) was synthesized. And a new kind of controllable photodegradable polystyrene (PS) composite was prepared by embedding the HADPG-TiO_2 into the commercial polystyrene. Solid-phase photocatalytic degradation of the PS-HADPG-TiO_2 composite was carried out in ambient air at room temperature under solar light irradiation. The HADPG-TiO_2 was characterized by FT-IR and scanning electron microscopy (SEM), X-ray diffraction (XRD) and UV–vis diffuse reflectance spectroscopy, in comparison with reference materials (plain TiO_2). The properties of PS-HADPG-TiO_2 films were compared with those of the pure PS films and PS-TiO_2 films by methods such as weight loss measurement, SEM and tensile properties measurement. The results showed that the HADPG-TiO_2 had a better dispersion in PS polymer and could absorb the visible light. The PS-HADPG-TiO_2 films had better tensile properties, compared with the pure PS films and PS-TiO_2 films. Moreover, the as-prepared PS-HADPG-TiO_2 films showed more excellent photostability under solar light irradiation for 0–250 h and higher photodegradable efficiency under the solar light irradiation for 600 h than the pure PS films and PS-TiO_2 films. The photocatalytic degradation mechanism of the films was briefly discussed. The novel fabrication method of composite polymer provides a valuable way for developing highly efficient and controllable photodegradable plastics.

1. Introduction

Polystyrene (PS) is widely used in our daily life and the modern plastic industry. However, PS and its related plastic products are non-biodegradable in natural environment. As PS recycling may neither be available nor economically viable, the large amount of the waste PS discarded is constantly increasing each year and is causing serious pollution problems. Traditional processing methods, such as garbage deposit or incineration, lead to a serious secondary pollution [1]. Therefore, the development of degradable PS plastics becomes an important issue.

Heterogeneous photocatalytic oxidation that can occur at moderate conditions has been widely used to deal with various pollutants [2–10]. Due to the characteristics such as inexpensiveness, good photostability, non-toxicity, and high-reactivity, TiO_2 has been generally regarded as the best photocatalyst. The photocatalytic degradation of PS by means of TiO_2 immobilized polystyrene (TiO_2-PS) has been proved an attractive and efficient technique for treatment of waste PS in open-air under UV light irradiation or solar exposure [11,12]. However, the poor dispersion of TiO_2 particles in PS matrix and low solar efficiency has already hindered the practical application of this technology. To eliminate these drawbacks, Zan et al. have investigated a novel photodegradable polystyrene-grafted-TiO_2 (PS-g-TiO_2) nanocomposite [13], which had a larger interface area and a higher photocatalytic activity. Some studies have developed a simple method for immobilization of TiO_2 nanoparticles on PS using a thermal attachment method [14,15], and this method made TiO_2 nanoparticles better dispersion in the surface of PS to greatly increase the photocatalytic efficiency of TiO_2. Fa et al.

* Corresponding author. Tel.: +86 0816 2419209.
E-mail address: leiyonglin@163.com (Y. Lei).

http://dx.doi.org/10.1016/j.polymdegradstab.2015.04.005
0141-3910/

have investigated the solid-phase photocatalytic degradation of PS films by embedding the iron phthalocyanine/TiO_2 nanoparticles into the commercial PS [16], the results showed that the photogradation of these films was significantly higher than that of the pure PS films and the PS-TiO_2 composite films both under the UV irradiation and under the sunlight irradiation. The solid-phase photodegradable efficiency of PS-TiO_2 was steadily enhanced after years of efforts. Nevertheless, proper stabilization of PS is essential to protect the physical and mechanical properties of PS from environmental impacts and to ensure a satisfactory lifetime. The addition of stabilizers, such as antioxidants and UV absorbers, is a common way to avoid degradation of PS by sun light [17–22]. This approach, however, synchronously causes the solid-phase photodegradable efficiency of PS-TiO_2 to greatly reduce. Therefore, the search for ways, to inhibit or at least retard photodegradation during the periods of service, and to accelerate photocatalytic degradation during the periods of disuse, is urgent for the further development of the technology based on photocatalytic degradation of PS-TiO_2 composite. However, A few researchers have recently studied how to balance photocatalytic degradation and light stabilization in PS.

In our previous works [23], the aromatic polyamide dendrimers modified TiO_2 hybrid photocatalyst (AD-TiO_2) was high power conversion efficiency and high molar extinction coefficient in the visible light range. Moreover, their thermal and chemical stability was better than that of PS, which ensured PS being degraded prior to aromatic polyamide dendrimers and maintained the visible photocatalytic efficiency of hybrid TiO_2 photocatalyst. Thence, we chose aromatic polyamide dendrimers to modify TiO_2 in order to improve the solid-phase visible photocatalytic degradation efficiency of PS.

Nowadays hindered amine stabilizers (HAS) are the most effective long-term light and partial heat stabilizers [24–29]. And the combination of HAS with UV absorber has been widely applied to improve the photostability of a variety of polymers [30–33]. AD-TiO_2 is not only excellent photocatalyst but also good UV absorber. However, instead of making the photostability of Ps better, the simply blending HAS with AD-TiO_2 makes the photostability of Ps worse because of the degradation and light stabilization of the PS emerging in different parts of the PS. So, taking a large number of $-NH_2$ groups of AD-TiO_2 that can be further reacted with $=O$ groups of Tetramethylpiperidinone into consideration, we introduced hindered amine into AD-TiO_2 to form the whole hindered amine structured photocatalyst. We expect that this structured photocatalyst can form stable nitroxide radicals by hindered amine capturing oxygen-centred alkoxy or peroxy radicals generated from TiO_2 photocatalytic interface during the periods of the service, which results in longer term photostability of PS. And after nitroxide radicals bond with other free radicals of PS-TiO_2 interface, they can act as light-harvesting molecules of TiO_2 photocatalyst and accelerate photocatalytic degradation of PS during the periods of disuse. Meanwhile, taking proper the dispersions of AD-TiO_2 into consideration, we grafted PS on surfaces of AD-TiO_2 according to the method of Zan et al. [13]. To our best knowledge, there is no research in the field of the photodegradable PS with hindered amine modified aromatic polyamide dendrimer/polystyrene-grafted-TiO_2 photocatalyst (HADPG-TiO_2) yet.

In this paper, a new kind of controllable photodegradable PS composite film was prepared using HADPG-TiO_2 as photocatalyst. The structure of photocatalyst is as shown in Scheme 1. The photodegradation performance has been investigated under solar light irradiation. The mechanism of the solid-phase controllable photocatalytic reaction was probed.

2. Experimental

2.1. Chemicals

Anatase TiO_2 nanoparticles (particle diameter 20 nm) were purchased from Beijing Nachen S&T Ltd. (Beijing, China). Commercial polystyrene (PS) particles were supplied by Zhanjiang Xinzhongmei Chemical Co. Ltd. Methacryloxy propyl trimethoxyl silane, Triacetoneamine, Phenylethylene, Azodiisobutyronitrile, Dicyclohexylcarbodide, 3,5-diaminobenzoic acid and 4-dimethylaminopyridine were obtained from Shanghai Chemical Reagents (Shanghai). All of the other reagents (analytical grade purity) were provided from Chengdu Chemical Reagent Factory (Chengdu).

2.2. Synthesis of HADPG-TiO_2

The synthesis route of HADPG-TiO_2 is shown in Fig. 1.

TiO_2 (0.5 mol) was dispersed in 50 mL dichloromethane under ultrasonic vibrations for 60 min, then 0.25 mol of dicyclohexylcarbodide, 0.02 mol of 4-dimethylaminopyridine, 0.1 mol of 3,5-diaminobenzoic acid, and 0.1 mol of methacryloxy propyl trimethoxyl silane were added dropwise into the above suspension under nitrogen and magnetic stirring. The formed CH_2Cl_2 suspension was stirred at room temperature for 10 h, centrifuged, filtered and washed three times with CH_2Cl_2. The obtained intermediate was dried at 60 °C under vacuum and designated as **1**.

The intermediate **1** was dispersed in 50 mL dichloromethane under ultrasonic vibrations for 60 min, then 0.75 mol of dicyclohexylcarbodide, 0.06 mol of 4-dimethylaminopyridine, and 0.6 mol of 3,5-diaminobenzoic acid were added dropwise into the above suspension under nitrogen and magnetic stirring. The formed CH_2Cl_2 suspension was stirred at room temperature for 16 h, centrifuged, filtered and washed three times with CH_2Cl_2. The obtained intermediate was dried at 60 °C under vacuum and designated as **2**.

The intermediate **2** was dispersed in 50 mL ethyl alcohol absolute under ultrasonic vibrations for 60 min, then 0.4 mol of triacetoneamine was added dropwise into the above suspension under nitrogen and magnetic stirring. The formed ethyl alcohol absolute suspension was refluxed with stirring for 22 h, centrifuged, filtered and washed three times with ethyl alcohol absolute. The obtained intermediate was dried at 60 °C under vacuum and designated as **3**.

The intermediate **3** was dispersed in 50 mL ethyl alcohol absolute under ultrasonic vibrations for 60 min. This suspension solution was added in a Wolff bottle, stirring at 35 °C for 2 h. Styrene (20 mL), in which 0.18 g of AIBN was dissolved, was added into the Wolff bottle and the mixture was refluxed with stirring for 24 h under nitrogen. After the reaction, the mixture was centrifuged and the obtained HADPG-TiO_2 was extracted three times with toluene and dried in vacuum at 110 °C. The HADPG-TiO_2 was stored at room temperature in the dark.

2.3. Preparation of PS composite films

10 g PS was dissolved in 50 mL dichloromethane under vigorous stirring for 2 h to obtain the PS solution. At the same time, The HADPG-TiO_2 (0.2 g) was dispersed uniformly into 20 mL dichloromethane by ultrasonic vibration for 20 min. Then the suspension was added to PS solution. The HADPG-TiO_2 catalyst content was 2.0% relative to the total mass of PS. The composite films were prepared by spreading the viscous solution on a slide glass surface (10 cm–10 cm) and dried in airtight system for 48 h at room temperature. The pure PS films and PS-TiO_2 films were also

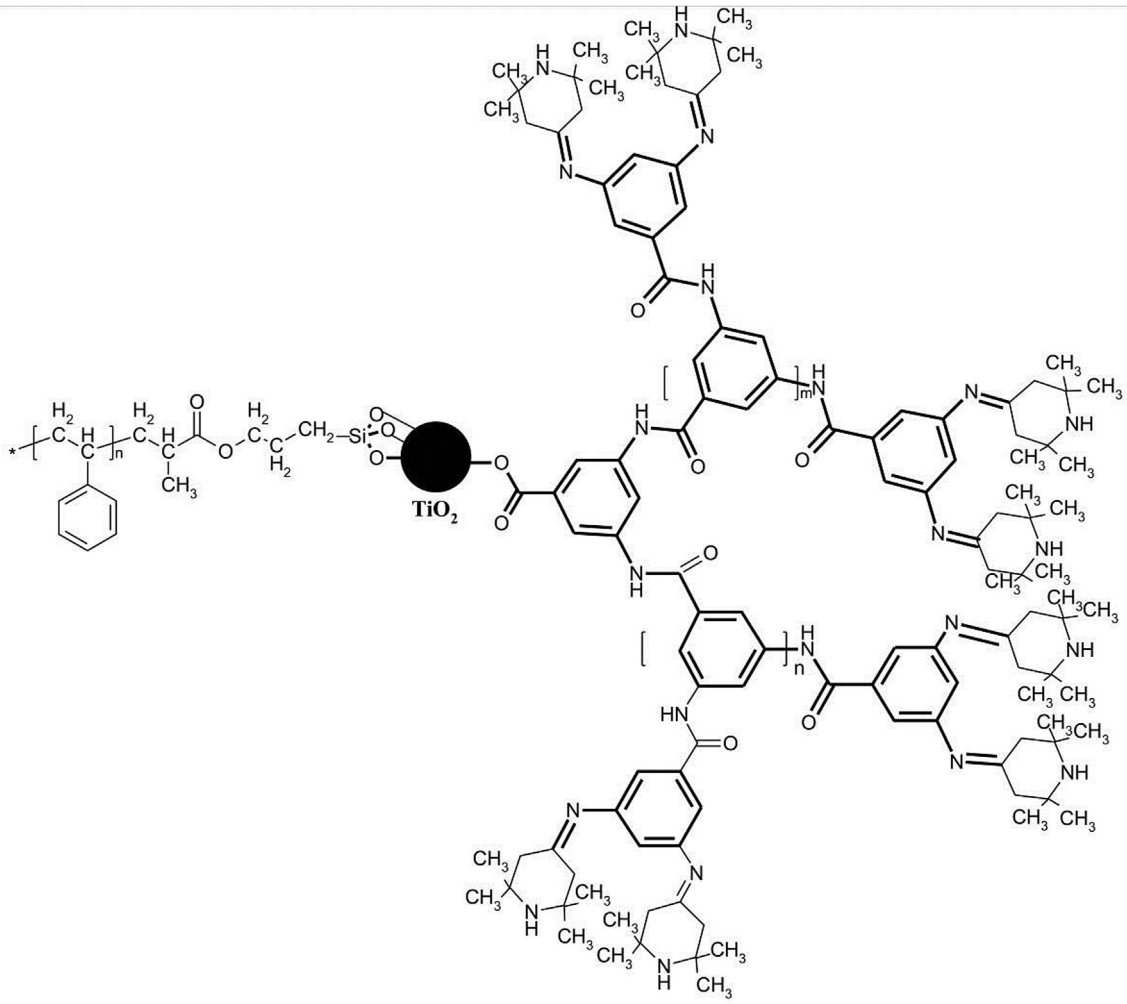

Scheme 1. Chemical structure of HADPG-TiO_2.

prepared in a similar procedure in order to compare the photocatalytic degradation activity and physical properties. The thickness of these films was measured about 0.1 mm by a micrometer.

2.4. Characterization

2.4.1. Characterization of photocatalysts

The crystalline phase of the photocatalysts was measured by X-ray diffraction (XRD, Cu Ka, 40 kV, 100 mA, Xpert MPD Pro). The surface morphologies of the photocatalysts were studied by field-emission scanning electron microscopy (FE-SEM, Ultra 55). Chemical structure information of the photocatalysts was collected using FT-IR spectra (VersionBM Spectrometer) with 2 cm^{-1} resolution using KBr pellet method. UV–vis diffuse reflectance spectra were recorded on a UV-3150 spectrophotometer equipped with an integrating sphere attachment.

2.4.2. Characterization of PS composite films

Tensile properties were determined from stress–strain curves with a Toyo Instron UTM-III-500 with a load cell of 10 kg at a drawing speed of 5 cm/min. Measurement was performed at 25 °C with film specimens (about 0.1 mm thick, 1.0 cm wide and 5-cm long) and average of at least five individual determinations was used. The surface morphologies were taken by field-emission scanning electron microscopy (Ultra 55).

2.5. Photocatalytic degradation of the composite films

The photocatalytic degradation was performed under solar light irradiation. The typical surface area of the film samples was 16 cm^2 (4 cm × 4 cm). Each film was washed several times with the deionized water and ultrasonic vibration to remove the traces of dichloromethane solvent before irradiation. The 16 cm^2 samples were placed in the quartz vessel on a terrace in sun-shining condition from the summer to the autumn. The average irradiation time was 5–8 h in 1 day. The weight loss was measured every 25 h. The surface morphologies of all samples after irradiation for 600 h were observed by field-emission scanning electron microscopy. Tensile properties of all samples after irradiation for 200 h and 600 h were also determined.

3. Results and discussion

3.1. Structural and optical characterization of HADPG-TiO_2

Fig. 2 shows the FT-IR spectra of plain TiO_2 and HADPG-TiO_2 hybrid particles. A wide absorption band at 450–750 cm^{-1} in Fig. 2a and b corresponds to the stretching vibration of Ti–O band and the absorption peaks at 3450, 1637 and 1399 cm^{-1} in Fig. 2a and b represent the stretching vibration and the in-plane bending vibration of surface hydroxyl groups. Based on the FT-IR result in

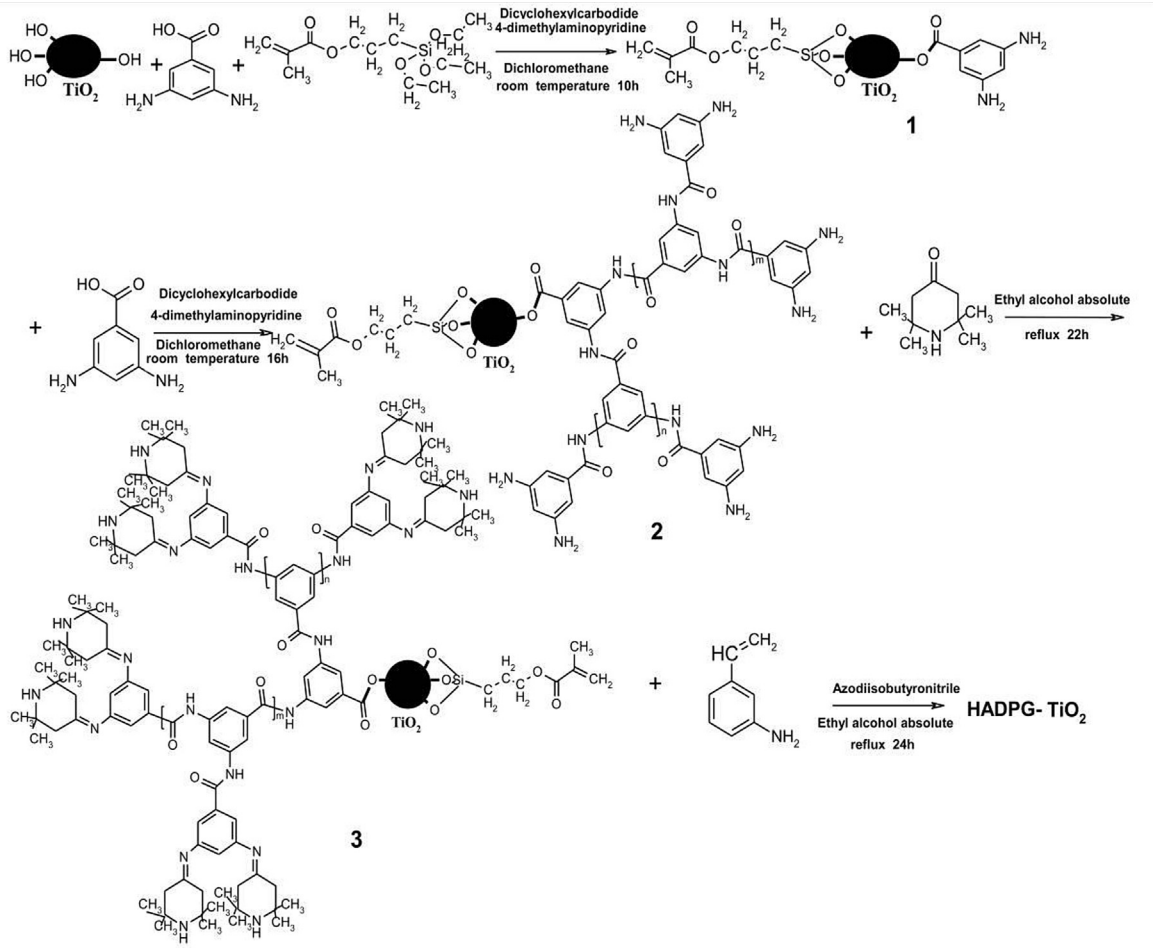

Fig. 1. Synthesis route of HADPG-TiO_2.

Fig. 2, new absorption peaks appear at 1496, 1450 cm^{-1} in FTIR spectrum of HADPG-TiO_2, which are the characteristic peaks of phenyl ring [34]. And the characteristic peaks of gem-dimethyl at 1220, 1180 cm^{-1} also appear. The new absorption peak at 2927 is assigned as C—H stretching mode. Moreover, a stronger and broader absorption at 3450 cm^{-1} and 1637 cm^{-1} in FTIR spectrum of HADPG-TiO_2 compared with plain TiO_2 are assigned to the stretching vibration of N—H and C=O,C=N symmetric stretching mode. These evidences proved the as-expected structures in Scheme 1 had occurred for HADPG-TiO_2.

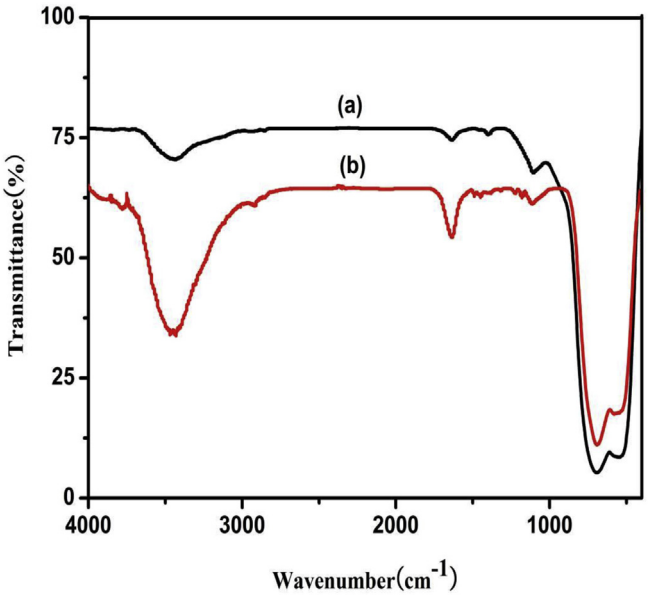

Fig. 2. FTIR spectra of (a) TiO_2 and (b) HADPG-TiO_2.

The XRD patterns of the plain TiO_2 and HADPG-TiO_2 hybrid particles are illustrated in Fig. 3. The peaks at $2\theta = 25.4°$, 37.7°, 48°, 53.8°, and 55.1° can be assigned to the diffractions of the (101), (004), (200), (105), and (211) crystal planes of anatase phase of TiO_2. It is also clear from the XRD patterns that the HADPG-TiO_2 remain almost the same as TiO_2. It indicated that the dominant structure of HADPG-TiO_2 was anatase, which would be very beneficial for the photocatalysis of the as-prepared hybrid photocatalyst.

Typical SEM images of TiO_2 and HADPG-TiO_2 particles are displayed in Fig. 4a and b. It can be observed that the plain TiO_2 nanoparticles are spherical, smooth, and strong aggregation. The average size of the TiO_2 nanoparticles is approximately 100 nm. The morphology of HADPG-TiO_2 particles does not differ much from that of plain TiO_2 and the average particles size is close to that of the plain TiO_2. However, the HADPG-TiO_2 particles appear with less aggregation and the surface of HADPG-TiO_2 particles is rougher than plain TiO_2.

The UV—vis DRS spectra of plain TiO_2 and HADPG-TiO_2 particles are shown in Fig. 5. It can be found that the plain TiO_2 can only absorb UV light ($\lambda < 387$ nm) and the HADPG-TiO_2 can absorb both UV light and visible light. The UV band from 200 to 400 nm of HADPG-TiO_2 is due to the absorption of TiO_2 and the visible light

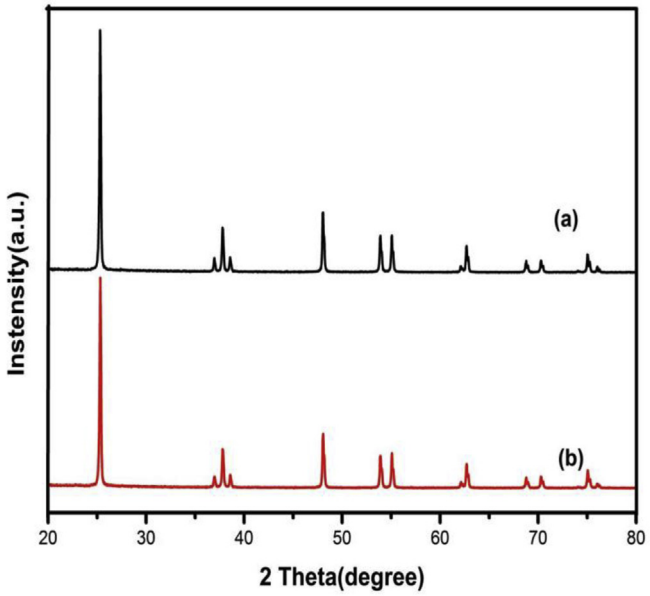

Fig. 3. XRD patterns of (a) TiO_2 and (b) HADPG-TiO_2.

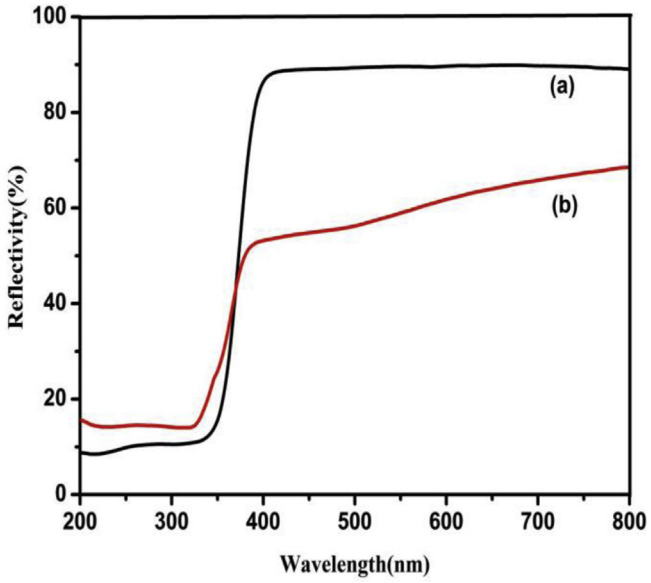

Fig. 5. UV–vis diffuse reflectance spectra of (a) TiO_2 and (b) HADPG-TiO_2.

absorption band between 400 nm and 800 nm can be assigned to the aromatic polyamide dendrimer structure of HADPG-TiO_2. Seen from Scheme 1, the aromatic polyamide dendrimer is of whole p conjugated structure and electron donor. And TiO_2 is electron acceptor due to its electron-deficient of d-orbital. When the aromatic polyamide dendrimer is bonded with TiO_2, the typical donor-acceptor type p conjugated structure forms. These donor-acceptor type chemical structures led to the decrease of the electron-transition energy and the improvement of visible light absorption.

3.2. Characterization of PS composite films

Tensile properties of pure PS films, PS-TiO_2 films and PS-HADPG-TiO_2 films were studied by the stress-strain analysis. The tensile strength and elongation at break were calculated and these values are given in Table 1.

The tensile strength and elongation at break in case of PS-HADPG-TiO_2 films were found to be higher than that of pure PS films and PS-TiO_2 films. Since the external stresses in a plastic composite were transferred from polymer matrix to the TiO_2 network, the tensile strength of the hybrid materials was dependent on the extent of bonding between the two phases and the surface area of the TiO_2. The PS-HADPG-TiO_2 films had the greater extent of bonding between the two phases and the more surface area of the TiO_2 particles than PS-TiO_2. These analysis can be confirmed by the SEM images of pure PS films, PS-TiO_2 films and PS-HADPG-TiO_2 films (Fig. 6). It can be seen from Fig. 6, the PS-TiO_2 films form micro size aggregates (Fig. 6b), which results in stress concentration points. And the nano TiO_2 particles of PS-HADPG-TiO_2 films are uniformly dispersed in PS matrix (Fig. 6c), which can make external stresses in PS-HADPG-TiO_2 films effectively transfer from polymer matrix to the TiO_2 network. Therefore, the PS-HADPG-TiO_2 films showed better tensile strength. The elongation at break of films was dependent on the dense extent of films. The SEM images of pure PS films and PS-TiO_2 films showed more holes and cracks than that of the PS-HADPG-TiO_2 films (Fig. 6). Thence, the elongation at break of the PS-HADPG-TiO_2 films was larger as compared to the pure PS films and PS-TiO_2 films.

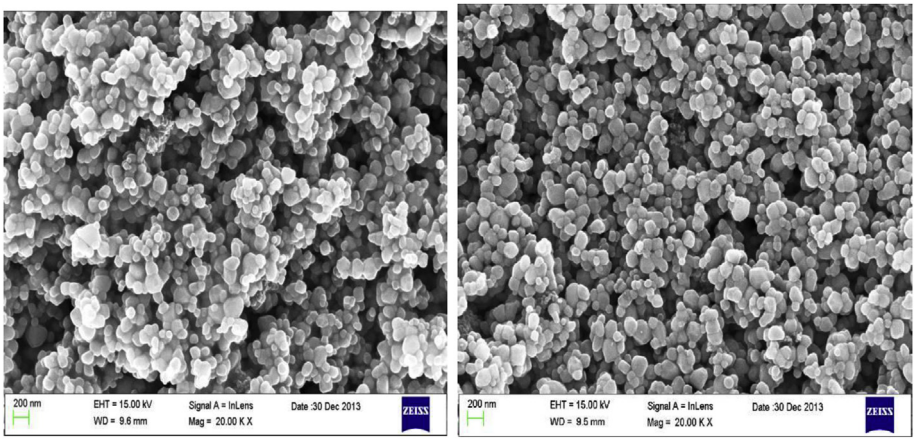

(a) **(b)**

Fig. 4. SEM images of (a) TiO_2 and (b) HADPG-TiO_2.

Table 1
The tensile strength and elongation at break of samples.

Samples	Tensile strength (MPa)	Elongation at break (%)
Pure PS	20.3	0.82
PS-TiO_2	19.1	0.84
PS-HADPG-TiO_2	25.3	1.18

3.3. Photocatalytic degradation of the PS composite films

The photoinduced weight loss of pure PS films, PS-TiO_2 films and PS-HADPG-TiO_2 films in air under solar light irradiation are shown in Fig. 7. The weight loss rate of the PS-HADPG-TiO_2 films was much greater than that of the pure PS films and PS-TiO_2 films. The weight loss of the pure PS films had almost no change in sunlight irradiation. This result reflects the fact that the pure PS is non-photodegradable in natural environment. The weight loss of the PS-TiO_2 films was only 9.53% under the solar light irradiation for 600 h, while that of the PS-HADPG-TiO_2 films reached 19.89%. It proved that the PS-HADPG-TiO_2 films had higher photodegradable efficiency than the PS-TiO_2 films under long-term sunlight exposure in natural environment. What's more, the weight of the PS-HADPG-TiO_2 films had almost no reduction under the solar light irradiation for 250 h and the weight loss of the PS-HADPG-TiO_2 films was the lowest in the three kinds of films. The weight loss of the PS-HADPG-TiO_2 films was only 1.11% under the solar light irradiation for 200 h, while that of the PS films reached 1.24%. The above weight loss data indicated that the PS-HADPG-TiO_2 films were indeed photodegradable with evident efficiency under long-term solar light irradiation in natural environment and had excellent photostability under short-term solar light irradiation.

In order to examine the service character of the solar irradiated polymer films, the tensile strength analysis of pure PS films, PS-TiO_2 films and PS-HADPG-TiO_2 films irradiated by sunlight for 200 h and 600 h in air was also carried out (Fig. 8). The tensile strength of the PS-HADPG-TiO_2 films was greater than that of the pure PS films and PS-TiO_2 films under the solar light irradiation for 200 h. This is the proof that addition of HADPG-TiO_2 into films can protect the mechanical properties of PS from solar irradiation impacts and ensure a satisfactory service lifetime. Moreover, after irradiated by sunlight for 600 h, the PS-HADPG-TiO_2 films had almost no tensile strength. This result can further support the fact that the photocatalytic degradation of PS for HADPG-TiO_2 is highly efficient under long-term solar light irradiation.

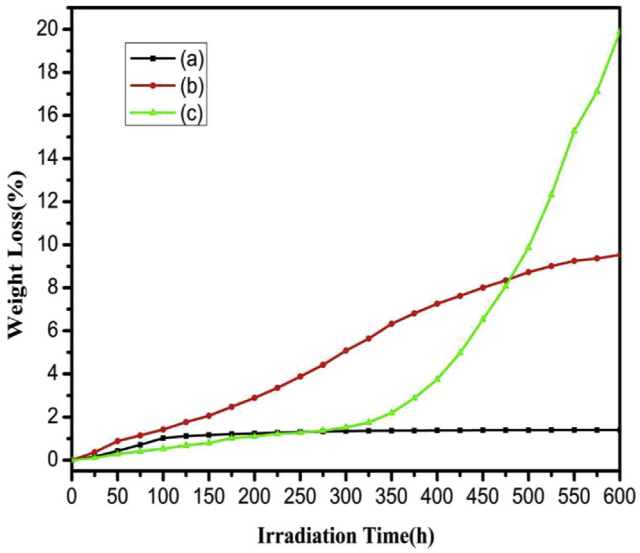

Fig. 7. The weight loss of films in air under solar light irradiation (a) pure PS films, (b) PS-TiO_2 films and (c) PS-HADPG-TiO_2 films.

The value of weight-average molecular weight (M_w) and polydispersity of pure PS, PS-TiO_2 and PS-HADPG-TiO_2 films after 0 h, 600 h of solar exposure are listed in Table 2. Before irradiation, M_w of pure Ps film was 46,670 g mol^{-1}, and after solar irradiation for 600 h, M_w of pure Ps film decreased by around 30%, while the M_w of PS-TiO_2 and PS-HADPG-TiO_2 films decreased respectively by around 75% and 85%. These results confirm the scission of polymer chain and formation of smaller molecules. After solar irradiation 600 h, M_w and the polydispersity values of PS-TiO_2 film were larger than that of PS-HADPG-TiO_2 films, as evidence that photodegradation using HADPG-TiO_2 promoted a higher concentration of small macromolecules than photodegradation using TiO_2 under long-term sunlight exposure in natural environment.

The surface morphologies of the films with photodegradation under the solar light irradiation for 600 h were also observed by SEM (Fig. 9). The SEM images revealed that the degradation of the PS matrix started from the PS—TiO_2 interface and led to the formation of cavities around TiO_2 particle aggregates (Fig. 9b and c), which are ascribed to the catalysis of TiO_2. After solar irradiated for 600 h, the PS-HADPG-TiO_2 films showed more degradation than the PS-TiO_2 films. On the other hand, only crystals formed on the

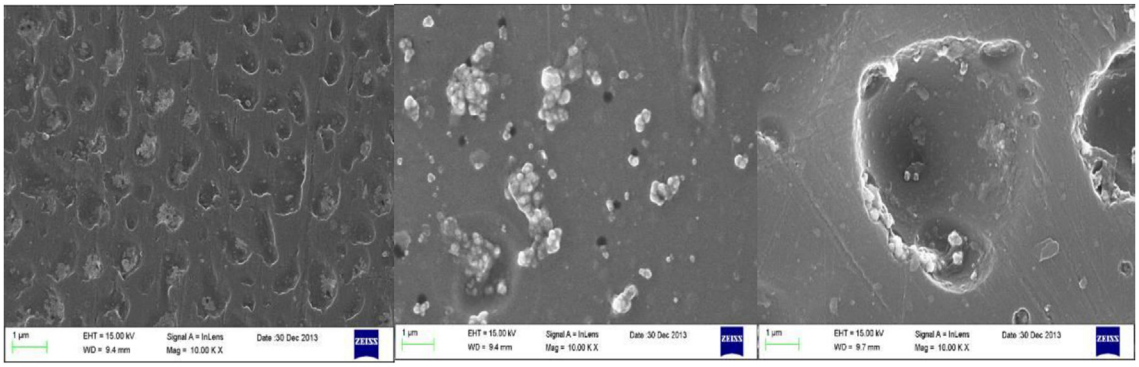

Fig. 6. SEM images of (a) pure PS films, (b) PS-TiO_2 films and (c) PS-HADPG-TiO_2 films.

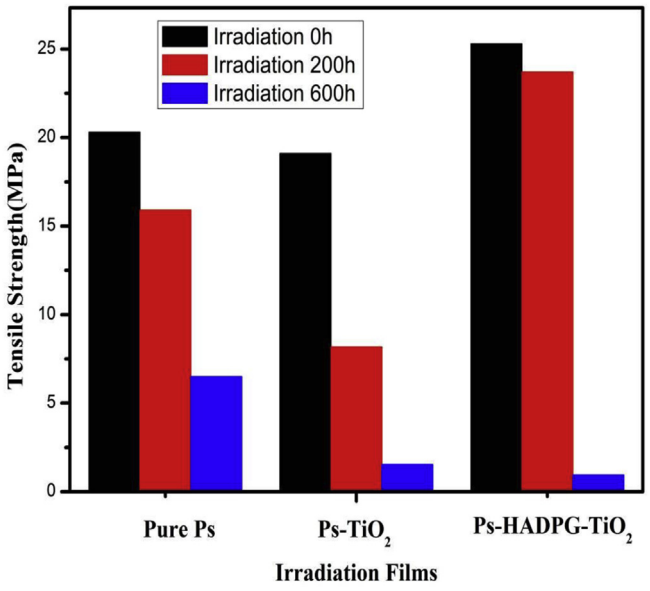

Fig. 8. The tensile strength of pure PS films, PS-TiO_2 films and PS-HADPG-TiO_2 films solar irradiated for 0 h, 200 h and 600 h in air.

Table 2
The molecular weight of pure PS films, PS-TiO_2 films and PS-HADPG-TiO_2 films solar irradiated for 0 h, 600 h in air.

Samples	M_w ($gmol^{-1}$)	Polydispersity (M_w/M_n)
Pure PS (0 h)	46,670	2.8
Pure PS (600 h)	33,695	2.5
PS-TiO_2 (600 h)	11,434	1.7
PS-HADPG-TiO_2 (600 h)	8307	1.4

irradiated surface of the pure PS films. These results are in accordance with the weight loss data shown in Fig. 7.

3.4. Degradation mechanism of the PS-HADPG-TiO_2 films

The as-prepared PS-HADPG-TiO_2 films showed excellent photostability under solar light irradiation for 0–250 h and highly efficient photodegradation under the solar light irradiation for 600 h. The photodegradation activity of the PS-HADPG-TiO_2 films was quite different from that of pure PS films and PS-TiO_2 films. The photodegradation mechanism of the PS-HADPG-TiO_2 films could be explained as follow (as shown in Scheme 2):

The linking of aromatic polyamide dendrimer to TiO_2 led to form donor-acceptor type p-conjugated surface complexes on TiO_2 surface that could be easily excited by sunlight. The electrons excited from p-conjugated surface complexes (donor) would inject into the unfilled d-orbital of Ti (acceptor), and then transferred into the conduction band of TiO_2 (Eq. (1)). These ligand-to-metal charge transfer (LMCT) processes were consistent with the reported works by other researchers [35–37]. The injected electron could reduce surface chemisorbed oxidants such as O_2 or H_2O to yield the $^1O_2$, $^*OH$ and O_2^- radicals (Eqs. (2)–(4)). These active oxygen radicals attacked the PS chains to form R* radicals and ROO* radicals (Eqs. (5)–(7)). As the PS-HADPG-TiO_2 films had a large number of hindered amine groups at the periphery of HADPG-TiO_2 hybrid photocatalyst, these active oxygen radicals could also react with hindered amine groups to form stable nitroxide radicals, and then the nitroxide radicals could bond with R* radicals and ROO* radicals to form stable ether and carbonyl compounds (Scheme 2). Above the process of free radicals scavenging by a large number of hindered amine groups occurred in the periods of the PS-HADPG-TiO_2 films irradiated by sunlight for 0–250 h. Hence, the PS-HADPG-TiO_2 films showed hard photodegradation under solar light irradiation for 0–250 h. After the PS-HADPG-TiO_2 films were irradiated by sunlight for 250 h, the reacted hindered amine groups could not scavenge polymer and oxygen radicals anymore. Simultaneously, the formed ether and carbonyl compounds could absorb UV radiation readily and acted as light-harvesting molecules in HADPG-TiO_2. As a result, the more active oxygen radicals occurred and easily attacked neighboring PS chains to form carbon centered radicals and carbonyl intermediates (Eqs. (8)–(10)). Finally, PS chains break [12] and CO_2 are evolved (Eq. (11)). Therefore, the HADPG-TiO_2 accelerated photocatalytic degradation of PS during the periods of the PS-HADPG-TiO_2 films irradiated by sunlight for 250–600 h. Photoinduced reaction steps in the HADPG-TiO_2 film may be as follow:

$$TiO_2 + h\lambda \rightarrow TiO_2^*\left(e_{cb}^- + h_{vb}^+\right) \quad (1)$$

$$e_{cb}^- + O_{2ads} \rightarrow O_2^- \quad (2)$$

$$TiO_2^* + O_{2ads} \rightarrow {}^1O_2 \quad (3)$$

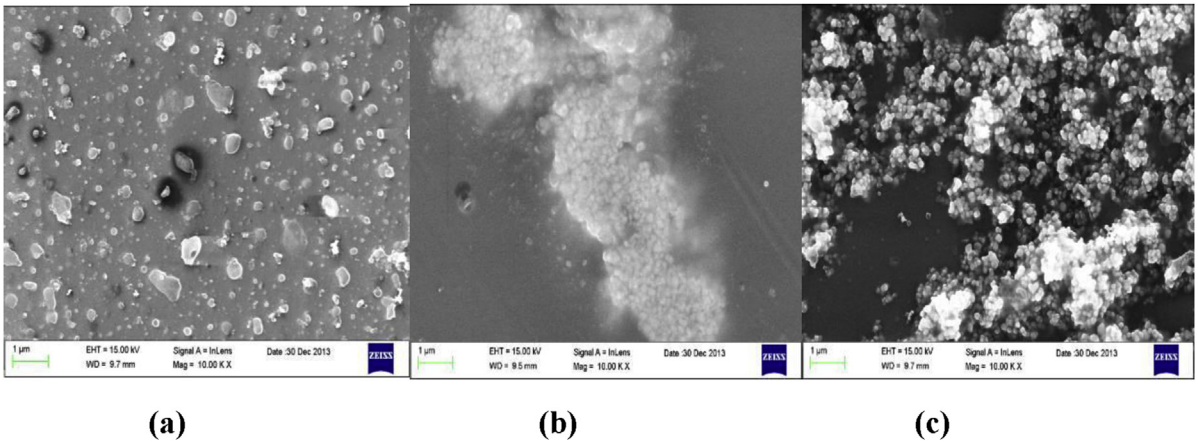

Fig. 9. SEM images of films under the solar irradiation for 600 h (a) pure PS films, (b) PS-TiO_2 films and (c) PS-HADPG-TiO_2 films.

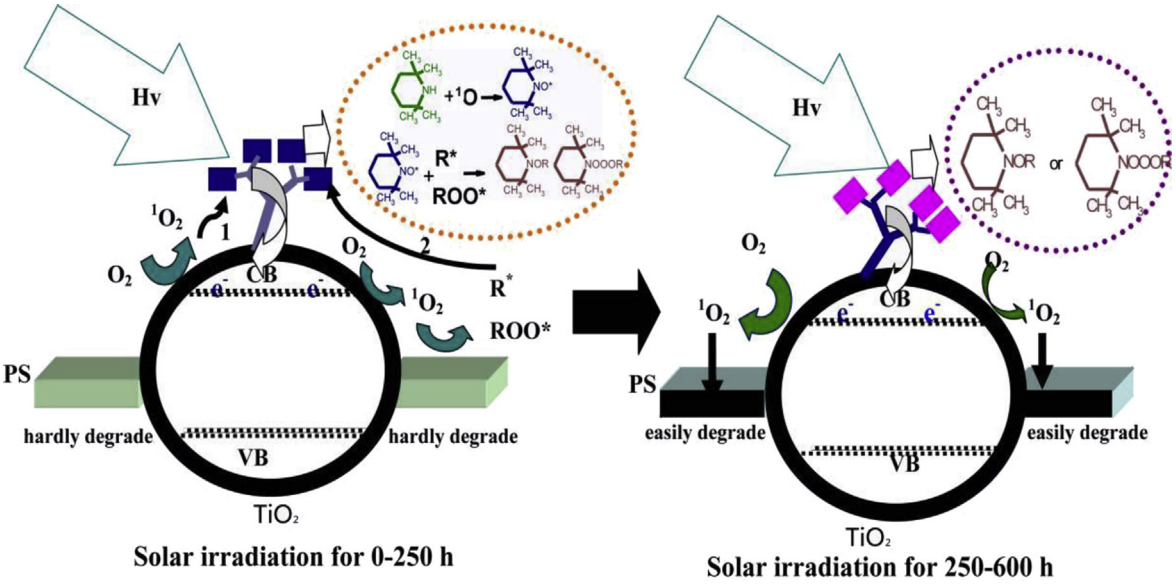

Scheme 2. Proposed photodegradation mechanism of the PS-HADPG-TiO_2 films.

$$H_2O_{ads} + h^+_{vb} \rightarrow {}^*OH + H^+ \quad (4)$$

$$-(CH_2CHC_6H_5) - + {}^*OH \rightarrow -(CH_2{}^*CC_6H_5) - + H_2O \quad (5)$$

$$-(CH_2{}^*CC_6H_5) - + {}^1O_2 \rightarrow -(CH_2{}^*CC_6H_5OO) - \quad (6)$$

$$-(CH_2{}^*CC_6H_5OO) - + O_2 \rightarrow -(CH_2COO{}^*C_6H_5OO) - \quad (7)$$

$$-(CH_2COO{}^*C_6H_5OO) - + -(CH_2CHC_6H_5) - \rightarrow -(CH_2COOHC_6H_5OO) - + -(CH_2{}^*CC_6H_5) - \quad (8)$$

$$-(CH_2COOHC_6H_5OO) - \rightarrow -(CH_2COC_6H_5OO) - + {}^*OH \quad (9)$$

$$-(CH_2COC_6H_5OO) - + O_2 \rightarrow R'COOH + R''COOH + \text{aldehydes and ethanol} \quad (10)$$

$$acid + \text{aldehydes and ethanol} \xrightarrow{h\lambda, TiO_2, O_2} \text{successive cleavage with } CO_2 \text{ evolution} \quad (11)$$

4. Conclusions

The HADPG-TiO_2 hybrid photocatalyst had better dispersion in PS polymer, possessed a large number of hindered amine groups at the periphery, and could absorb the visible light. So the PS-HADPG-TiO_2 films had better tensile properties, compared with the pure PS films and PS-TiO_2 films. What's more, the as-prepared PS-HADPG-TiO_2 films showed more excellent photostability under solar light irradiation for 0–250 h and higher photodegradable efficiency under the solar light irradiation for 600 h than the pure PS films and PS-TiO_2 films. The weight loss of the PS-HADPG-TiO_2 films was only 1.11% under the solar light irradiation for 200 h, while that of the PS films reached 1.24%. The weight loss of the PS-TiO_2 films was only 9.53% under the solar light irradiation for 600 h, while that of the PS-HADPG-TiO_2 films reached 19.89%. The hindered amine captured $^1O_2$ radicals, R* and ROO* radicals in clarifying why the PS-HADPG-TiO_2 films showed hard photodegradation under solar light irradiation for 0–250 h. And the reacted hindered amine groups could absorb UV radiation readily and acted as light-harvesting molecules in HADPG-TiO_2 in clarifying why the HADPG-TiO_2 accelerated photocatalytic degradation of PS during the periods of the PS-HADPG-TiO_2 films irradiated by sunlight for 250–600 h. On the basis of this present investigation, the novel fabrication method of composite polymer provides a valuable way for developing highly efficient and controllable photodegradable plastics.

Acknowledgments

This work was supported by Engineering Research Center Of Biomass Materials, Ministry of Education, China (Grant No. 13zxbk05).

References

[1] Takasuga T, Makino T, Tsubota K, Takeda N. Formation of dioxins (PCDDs/PCDFs) by dioxin-free fly ash as a catalyst and relation with several chlorine-sources. Chemosphere 2000;40:1003–7.
[2] Alrousan DMA, Dunlop PSM, McMurray TA, Byrne JA. Photocatalytic inactivation of *E. coli* in surface water using immobilised nanoparticle TiO_2 films. Water Res 2009;43:47–54.
[3] Caballero L, Whitehead KA, Allen NS, Verran J. Inactivation of *Escherichia coli* on immobilized TiO_2 using fluorescent light. J Photochem Photobiol A 2009;202:92–8.
[4] Calza P, Avetta P, Rubulotta G, Sangermano M, Laurenti E. Photocatalytic degradation of phenolic compounds with new TiO_2 catalysts. Chem Eng J 2014;239:87–92.
[5] Chang H, Jo EH, Jang HD, Kim TO. Synthesis of PEG-modified TiO_2–$InVO_4$ nanoparticles via combustion method and photocatalytic degradation of methyleneblue. Mater Lett 2013;92:202–5.
[6] Chun HH, Jo WK. Polymer material-supported titania nanofibers with different polyvinylpyrrolidone to TiO_2 ratios for degradation of vaporous trichloroethylene. J Ind Eng Chem 2014;20:1010–5.
[7] Qin GH, Zhang Y, Ke XB, Tong XL, Sun Z, Liang M, et al. Photocatalytic reduction of carbon dioxide to formic acid, formaldehyde, and methanol using dye-sensitized TiO_2 film. Appl Catal B 2013;129:599–605.
[8] Bianchi CL, Gatto S, Pirola C, Naldoni A, Michele AD, Cerrato G, et al. Photocatalytic degradation of acetone, acetaldehyde and toluene ingas-phase: comparison between nano and micro-sized TiO_2. Appl Catal B 2014;146:123–30.
[9] Liu GL, Zhu DW, Liao SJ, Ren LY, Cui JZ, Zhou WB. Solid-phase photocatalytic degradation of polyethylene–goethite composite film under UV-light irradiation. J Hazard Mater 2009;172:1424–9.

[10] Thomas RT, Nair V, Sandhyarani N. TiO_2 nanoparticle assisted solid phase photocatalytic degradation of polythene film: a mechanistic investigation. Colloid Surf A 2013;422:1–9.
[11] Shang J, Chai M, Zhu Y. Photodegradation of polystyrene plastic under fluorescent light. Environ Sci Technol 2003;37:4494–9.
[12] Shang J, Chai M, Zhu Y. Solid-phase photocatalytic degradation of polystyrene plastic with TiO_2 as photocatalyst. J Solid State Chem 2003;174:104–10.
[13] Zan L, Wang SL, Fa WJ, Hu YH, Tian LH, Deng KJ. Solid-phase photocatalytic degradation of polystyrene with modified nano-TiO_2 catalyst. Polymer 2006;47:8155–62.
[14] Fabiyi ME, Skelton RL. Photocatalytic mineralisation of methylene blue using buoyant TiO_2-coated polystyrene beads. J Photochem Photobiol A 2000;132:121–8.
[15] Altın I, Sökmen M. Preparation of TiO_2-polystyrene photocatalyst from waste material and its usability for removal of various pollutants. Appl Catal B 2014;144:694–701.
[16] Fa W, Zan L, Gong C, Zhong J, Deng K. Solid-phase photocatalytic degradation of polystyrene with TiO_2 modified by iron (II) phthalocyanine. Appl Catal B 2008;79:216–23.
[17] Chen T, Zhu L, Liu X, Li Y, Zhao C, Xu Z, et al. Synthesis and antioxidant activity of phosphorylated polysaccharide from *Portulaca oleracea* L. with $H_3PW_{12}O_{40}$ immobilized on polyamine functionalized polystyrene bead as catalyst. J Mol Catal A 2011;342–343:74–82.
[18] Grelier S, Castellan A, Podgorski L. Use of low molecular weight modified polystyrene to prevent photodegradation of clear soft woods for outdoor use. Polym Degrad Stab 2007;92:1520–7.
[19] Hess DB, Muller SJ. Secondary effects of antioxidant on PS/PVME blends. Polymer 2002;43:1567–70.
[20] Samoladas A, Bikiaris D, Zorba T, Paraskevopoulos KM, Jannakoudakis A. Photochromic behavior of spiropyran in polystyrene and polycaprolactone thin films – effect of UV absorber and antioxidant compound. Dyes Pigm 2008;76:386–93.
[21] Rabie ST, Ahmed AE, Sabaa MW, Ghaffar MAA. Maleic diamides as photostabilizers for polystyrene. J Ind Eng Chem 2013;19:1869–78.
[22] Yousif E, Salimon J, Salih N. New stabilizers for polystyrene based on 2-N-salicylidene-5-(substituted)-1,3,4-thiadiazole compounds. J Saudi Chem Soc 2012;16:299–306.
[23] Lei YL, Zhang C, Lei H, Huo JC. Visible light photocatalytic activity of aromatic polyamide dendrimer/TiO_2 composites functionalized with spirolactam-based molecular switch. J Colloid Interface Sci 2013;406:178–85.
[24] Motyakin MV, Schlick S. Thermal degradation at 393 K of poly(acrylonitrile-butadiene-styrene) (ABS) containing a hindered amine stabilizer: a study by 1D and 2D electron spin resonance imaging (ESRI) and ATR–FTIR. Polym Degrad Stab 2002;76:25–36.
[25] Balabanovich AI, Klimovtsovaa IA, Prokopovich VP, Prokopchuk NR. Thermal stability and thermal decomposition study of hindered amine light stabilizers. Thermochim Acta 2007;459:1–8.
[26] Ackermann L, Sandmann R, Schinkel M, Kondrashov MV. Palladium-catalyzed sequential indole synthesis using sterically hindered amines. Tetrahedron 2009;65:8930–9.
[27] Gijsman P, Smelt HJ, Schumann D. Hindered amine light stabilizers: an alternative for radiation cross-linked UHMWPE implants. Biomaterials 2010;31:6685–91.
[28] Feczkó T, Kovács M, Voncina B. Improvement of fatigue resistance of spirooxazine in ethyl cellulose and poly(methyl methacrylate) nanoparticles using a hindered amine light stabilizer. J Photochem Photobiol A 2012;247:1–7.
[29] Evans PD, Gibson SK, Cullis I, Liu C, Sèbe G. Photostabilization of wood using low molecular weight phenol formaldehyde resin and hindered amine light stabilizer. Polym Degrad Stab 2013;98:158–68.
[30] Bojinov VB, Panova IP. Photo-stability of yellow-green emitting 1,8-naphthalimides containing built-in s-triazine UV absorber and HALS fragments and their acrylonitrile copolymers. Polym Degrad Stab 2008;93:1142–50.
[31] Bojinov VB, Panova IP, Simeonov DB. The synthesis of novel photostable fluorescein-based dyes containing an s-triazine UV absorber and a HALS unit and their acrylonitrile copolymers. Dyes Pigm 2009;83:135–43.
[32] Bojinov VB, Panova IP, Simeonov DB, Georgiev NI. Synthesis and sensor activity of photostable blue emitting 1,8-naphthalimides containing s-triazine UV absorber and HALS fragments. J Photochem Photobiol A 2010;210:89–99.
[33] Danko M, Hrdlovič P, Chmela Š. The photolysis in polymer matrices of dyes containing a benzothioxanthene chromophore linked with a hindered amine. Polym Degrad Stab 2011;96:1955–60.
[34] Takurou NM, Yoshinori F, Yoshiaki H, Yoshikazu T, Mitsuo T, Norimichi K. Surface modification of polystyrene and poly(methyl methacrylate) by active oxygen treatment. Colloid Surf B 2003;29:171–9.
[35] Jiang D, Xu Y, Wua D, Sun YH. Isocyanate-modified TiO_2 visible-light-activated photocatalyst. Appl Catal B 2009;88:165–72.
[36] Kim G, Choi W. Charge-transfer surface complex of EDTA-TiO_2 and its effect on photocatalysis under visible light. Appl Catal B 2010;100:77–83.
[37] Zhang X, Wu F, Deng NS. Efficient photodegradation of dyes using light-induced self assembly TiO_2/β-cyclodextrin hybrid nanoparticles under visible light. J Hazard Mater 2011;185:117–23.